

# **LG EXCITATION, ATTENUATION AND SOURCE SPECTRAL SCALING IN CENTRAL ASIA AND CHINA**

**J. Xie<sup>1</sup>  
L. Cong<sup>2</sup>  
B. J. Mitchell<sup>2</sup>**

AFOSR-TR-96

C107

**<sup>1</sup> Lamont-Doherty Earth Observatory  
of Columbia University  
Route 9W  
Palisades, NY 10964**

**<sup>2</sup> Department of Earth and Atmospheric Sciences  
3507 Laclede Ave.  
St. Louis University  
St. Louis, MO 63103**

**5 January 1996**

**Final Technical Report  
November 1, 1993 - October 31, 1995**

**Approved for public release; distribution unlimited.**

**AFOSR  
110 Duncan Ave.  
Suite B115  
Bolling AFB, DC 20332-0001**

**19960320 043**

**DTIC QUALITY INSPECTED 1**

REPORT DOCUMENTATION PAGE			Form Approved OMB No. 0704-0188	
Public reporting burden for this collection of information is estimated to average 1 hour per response, including the time for reviewing instructions, searching existing data sources, gathering and maintaining the data needed, and completing and reviewing the collection of information. Send comments regarding this burden estimate or any other aspect of this collection of information, including suggestions for reducing this burden, to Washington Headquarters Services, Directorate for Information Operations and Reports, 1215 Jefferson Davis Highway, Suite 1204, Arlington, VA 22202-4302, and to the Office of Management and Budget, Paperwork Reduction Project (0704-0188), Washington, DC 20503.				
1. AGENCY USE ONLY (Leave blank)		2. REPORT DATE		3. REPORT TYPE AND DATES COVERED Final Technical 11/1/93-10/31/95
4. TITLE AND SUBTITLE Lg excitation, attenuation and source spectral scaling in central Asia and China			5. FUNDING NUMBERS F49620-94-1-0025	
6. AUTHOR(S) J. Xie                      L. Cong                      B. J. Mitchell				
7. PERFORMING ORGANIZATION NAME(S) AND ADDRESS(ES) Dept. of Earth & Atmospheric Sciences Saint Louis University 3507 Laclede St. Louis, MO 63103			8. PERFORMING ORGANIZATION REPORT NUMBER	
9. SPONSORING/MONITORING AGENCY NAME(S) AND ADDRESS(ES) AFOSR/NM 110 Duncan Avenue, Suite B115 Bolling AFB, DC20332-0001			10. SPONSORING/MONITORING AGENCY REPORT NUMBER	
11. SUPPLEMENTARY NOTES				
12a. DISTRIBUTION/AVAILABILITY STATEMENT			12b. DISTRIBUTION CODE	
13. ABSTRACT (Maximum 200 words)  The non-linear inverse method of Xie (1993) is applied to analyze Lg spectra from 21 underground nuclear explosions and 52 shallow (5-33 km) earthquakes in central Eurasia where, for numerous paths, Lg Q and Lg coda Q at 1 Hz are found to be very similar. The logarithm of Lg seismic moment ( $M_0$ ) values correlate linearly with body-wave magnitude ( $M_b$ ), with slopes of slightly greater than 1.0. For the same $M_0$ values, the $M_b$ values for earthquakes tend to be systematically lower than those for explosions. For both explosions and earthquakes, $M_0$ scale with $f_c^{-\alpha}$ , with $f_c$ being Lg corner frequency and $\alpha$ being closer to 4 than to 3. For explosions, the estimated $M_0$ , $f_c$ values are dependent on whether the explosion or earthquake source model is used. At any given $M_0$ level, the $f_c$ value estimated for an explosion with the <i>earthquake</i> source model tends to be higher than that for an earthquake. This tendency appears to be opposite to that observed at the NTS, and maybe used as an explosion discriminant for central Eurasia.				
14. SUBJECT TERMS Attenuation    Lg excitation    Nuclear explosions Source spectral scaling    Seismic moment    Corner frequency			15. NUMBER OF PAGES 30	
			16. PRICE CODE	
17. SECURITY CLASSIFICATION OF REPORT unclassified	18. SECURITY CLASSIFICATION OF THIS PAGE unclassified	19. SECURITY CLASSIFICATION OF ABSTRACT unclassified	20. LIMITATION OF ABSTRACT unclassified	

## TABLE OF CONTENTS

I.	ABSTRACT .....	1
II.	STATEMENT OF WORK.....	3
III.	RESEARCH ACCOMPLISHED .....	4
	Data processing .....	4
	Agreements among 1 Hz Q measured using Lg from explosions, Lg from earthquakes and Lg coda .....	15
	Comparison between Lg $\eta$ and Lg coda $\eta$ .....	16
	Correlation between $M_0$ (Lg) and ISC $M_b$ .....	18
	Previously unresolved issues on the scaling between $M_0$ and $f_c$ values....	19
	Scaling between $M_0$ and $f_c$ values for explosions .....	20
	Scaling between $M_0$ and $f_c$ values for earthquakes .....	23
	Dependence of $M_0$ , $f_c$ estimates on theoretical source models .....	23
	Comparison between $M_0$ - $f_c$ scalings for earthquakes and explosions .....	24
	Implications on the difference between excitations of local S and Lg.....	25
IV.	FUTURE RESEARCH .....	25
V.	REFERENCES.....	26
VI.	PUBLICATIONS .....	29
VII.	PROFESSIONAL PERSONNEL.....	29
VIII.	PAPERS PRESENTED AT MEETINGS.....	29

## LIST OF TABLES AND FIGURES

Table 1 .....	5
Table 2 .....	6
Figure 1 .....	7
Figure 2 .....	8
Figure 3 .....	9
Figure 4 .....	10
Figure 5(a).....	11
Figure 5(b).....	12
Figure 5(c).....	13
Figure 6 .....	14
Figure 7 .....	17
Figure 8 .....	21
Figure 9 .....	22

# LG EXCITATION, ATTENUATION AND SOURCE SPECTRAL SCALING IN CENTRAL ASIA AND CHINA

Jiakang Xie, Lianli Cong and B.J. Mitchell

Department of Earth and Atmospheric Sciences, St. Louis University

3507 Laclede Ave., St. Louis, MO 63103

## I. ABSTRACT

The non-linear inverse method of Xie (1993) is applied to analyze Lg spectra from 21 recent underground nuclear explosions and 52 shallow (5-33 km) earthquakes in central Eurasia. The data set used in this study consists hundreds of high-quality Lg spectra, collected from broad-band IRIS, CDSN and KNET stations. For those events from which Lg spectra at multiple ( $\geq 3$ ) stations are available, the analyses simultaneously determine the Lg seismic moments ( $M_0$ ), corner frequencies ( $f_c$ ), path-variable Lg Q values at 1 Hz and their frequency dependences. For the events with Lg spectra recorded at only one or two stations, the analyses typically only determine Lg  $M_0$  and  $f_c$  values, with path Lg Q values fixed using *a priori* information obtained from earlier inversions. The main findings of this study include

- (1) Lg Q values at 1 Hz for numerous paths in central Eurasia generally agree well with those predicted using a tomographic Lg coda Q map (Xie & Mitchell, 1991). This suggests that the 1 Hz Lg Q values obtained in this inversion have not been significantly biased by effects of non-isotropic source radiation patterns or large-scale 3D structural complications. The power-law frequency dependences of Lg Q and Lg coda Q also agree at distances between about 800 and 2700 km. At larger distances the Lg Q tends to show low ( $\sim 0.0$ ) frequency dependence.
- (2) For both underground nuclear explosions and the earthquakes studied, the logarithm of Lg  $M_0$  values correlate linearly with the ISC body wave magnitude ( $M_b$ ), with slopes of slightly greater than 1.0. For the same  $M_0$  values,  $M_b$  values for the earthquakes tend to be systematically lower than for the explosions.
- (3) For the 21 underground nuclear explosions, the Lg  $M_0$  values estimated using the explosion source model (*i.e.*, the model with an overshoot effect) scale with  $f_c^{-4}$ , instead with  $f_c^{-3}$ , as predicted by a constant stress drop scaling relationship.
- (4) For the earthquakes, the Lg  $M_0$  values estimated using the earthquake source model (*i.e.*, the  $\omega^2$  model without overshoot) scale with  $f_c^{-\alpha}$ , with the value of  $\alpha$  being about 3.6 when all of the 53 earthquakes are used in a regression analysis, and about

4.0 when only the well-recorded earthquakes (*i.e.*, the earthquakes with Lg spectra recorded at three or more stations) are used.

- (5) To simulate a situation in which we do not know that the explosions are explosions, we also inverted for their Lg  $M_0$  and  $f_c$  values using the *earthquake* source model. The Lg  $M_0$  and  $f_c$  values thus estimated are systematically different from those estimated for the explosions using the *explosion* source model: for the same  $f_c$  values, the Lg  $M_0$  values estimated using the explosion source model is systematically lower (by a factor of 0.27) than those estimated using the earthquake source model. This factor indicates that there is a strong model-dependence in the estimated Lg  $M_0$  and  $f_c$  values when the Lg from explosions is studied.
- (6) The scaling between Lg  $M_0$  and  $f_c$  values for the explosions, estimated using the *earthquake* source model, also differ from that between the Lg  $M_0$  and  $f_c$  values for the earthquakes. The main difference between the two scalings is that for a given  $M_0$ , the explosions tend to have higher  $f_c$  values. This suggests that the Lg from explosions has a richer high-frequency content, as compared to Lg from earthquakes. This phenomenon appears to be systematic in central Eurasia, and appear to be opposite to that observed in the western U.S. It is therefore highly recommended that more research be conducted on which of these phenomena is more common for various continental environments.

## II. STATEMENT OF WORK

Xie (1993) developed a non-linear inverse method for simultaneously estimating Lg source spectral parameters and path-variable Lg Q values. The advantages of that method, including its requiring no starting model for the unknown parameters and its allowing Lg Q to be path-variable, are fully described in Xie (1993). The proposed work for this two-year research is to apply the method of Xie (1993) to broad-band Lg records from many underground nuclear explosions and earthquakes occurring in central Asia after late 1987, the time when installations of broad-band stations began in Eurasia. The proposed steps of this study are:

- (1) Determine path variable  $Q_0$  and  $\eta$  ( Lg Q at 1 hz and its power-law frequency dependence; defined via  $Q(f) = Q_0 f^\eta$ ) values from the Balapan and Lop Nor test sites to the recently installed broad-band seismic stations in Eurasia.
- (2) Compare the resulting  $Q_0$  and  $\eta$  values with those predicted using the tomographic Lg coda Q map (Xie & Mitchell, 1991; Pan *et al.*, 1992). Find if these values disagree due to effects of either abnormal attenuation of Lg or Lg coda caused by large-scale 3D structural complications, or non-isotropic radiation patterns by the seismic sources.
- (3) Determine source spectral parameters, including seismic moment ( $M_0$ ) and corner frequency ( $f_c$ ), for explosions using the modified Mueller-Murphy source model, which is characterized by an  $\omega^{-2}$  high-frequency asymptote and an overshoot effect:

$$S^{\text{exp}}(f) = \frac{M_0}{4\pi\rho v_s^3} \frac{1}{\left[1 + (1 - 2\beta)f^2/f_c^2 + \beta^2 f^4/f_c^4\right]^{1/2}} \quad (1)$$

(Serenio *et al.*, 1988; Xie, 1993) . Determine the scaling between the resulting  $M_0$  and  $f_c$  values.

- (4) Determine  $M_0$  and  $f_c$  values for earthquakes using the  $\omega^{-2}$  earthquake source model with no overshoot effect:

$$S^{\text{eq}}(f) = \frac{M_0}{4\pi\rho v_s^3} \frac{1}{1 + f^2/f_c^2} \quad (2)$$

(Street *et al.*, 1975; Xie, 1993). Determine the scaling between the resulting  $M_0$  and  $f_c$  values.

- (5) From the results of (3) and (4), determine if  $M_0$  scales with  $f_c^{-3}$  or  $f_c^{-4}$  for explosions and earthquakes, and infer the resulting Lg source spectral scaling in terms of any fundamental differences between the excitation of Lg and that of local S waves by

both types of seismic sources (*i.e.*, to infer if the transfer function between the Lg and S excitations is flat; for details, *cf.* later sections).

- (6) Determine the  $M_0$  and  $f_c$  values for explosions using the *earthquake* source model, thus simulating a situation when we do not know that the events are explosions. Determine the scaling between the resulting  $M_0$  and  $f_c$  values.
- (7) Compare the the scaling derived in step (6) with that obtained in step (4) to see the difference between the  $M_0 - f_c$  scalings for explosions and earthquakes, both derived using the earthquake source model. Determine if the difference can be used as an effective discriminant of explosions.

### III. RESEARCH ACCOMPLISHED

Over the past two years we have collected hundreds of Lg spectra from 21 underground nuclear explosions and 53 shallow (5-33 km) earthquakes in/around the Balapan and Lop Nor test sites, recorded by 21 broad-band IRIS, CDSN and KNET stations. All events studied occurred after 1987, the time when the installation of broad-band digital stations began in Eurasia. Tables 1 and 2 lists the explosions and earthquakes studied, respectively. Figure 1 shows the locations of the events and stations used in this study. The earthquakes are chosen to be either near the test sites, or near the KNET stations, so that the source locations or paths involved in studying the earthquakes are similar to those involved in studying the explosions. The lengths of the paths used in this study are between about 800 km and 4045 km (see Figures 5a through 6).

#### Data processing

The Lg spectra are obtained in the same way as that described by Xie (1993). Figure 2 shows an example of the Lg time series, the 20% taper window used, and the resulting Lg spectra. For each event studied, we used the non-linear inverse method by Xie (1993) to invert for source and path spectral parameters. When the event is recorded by a sufficient number of stations ( $\geq 3$ ), we simultaneously inverted for source  $M_0$ ,  $f_c$  and path  $Q_0$ ,  $\eta$  values with no *a priori* information. For the events that are recorded by only one or two stations, we found that the information contained in the Lg spectra is typically not sufficient to constrain a simultaneous inversion and accordingly, for most of these events we used *a priori* information on path  $Q_0$  and  $\eta$  values obtained in the earlier simultaneous inversions. Figures 3 and 4 show examples of the fit of the optimal source/path parameters to the observed Lg spectra, where the inverted  $Q_0$ ,  $\eta$  values for multiple stations that recorded an explosion (Figure 3) and earthquake (Figure 4) are used to remove path



**Table 1. Underground Nuclear Explosions Studied†**

Event Date	Origin Time	$m_b$	Test Site	Seismic Moment (Nm)	Corner Frequency	Number of Stations Used
Dec. 27, 87	03H05M04.9S	6.1	Balapan	$1.3 (\pm 0.3) \times 10^{16}$	$0.61 \pm 0.04$ Hz	2
Feb. 13, 88	03H05M05.9S	6.1	Balapan	$1.7 (\pm 0.6) \times 10^{16}$	$0.62 \pm 0.05$ Hz	1
Apr. 3, 88	01H33M05.8S	6.0	Balapan	$1.7 (\pm 0.3) \times 10^{16}$	$0.59 \pm 0.04$ Hz	2
May 4, 88	00H57M06.8S	6.1	Balapan	$1.9 (\pm 0.6) \times 10^{16}$	$0.59 \pm 0.05$ Hz	1
Jun. 14, 88	02H27M06.4S	5.1	Balapan	$7.0 (\pm 3.4) \times 10^{14}$	$1.20 \pm 0.11$ Hz	1
Sep. 14, 88*	03H59M57.6S	6.1	Balapan	$1.3 (\pm 0.1) \times 10^{16}$	$0.56 \pm 0.02$ Hz	5
Nov. 12, 88	03H30M30.8S	5.4	Balapan	$2.6 (\pm 0.3) \times 10^{15}$	$0.82 \pm 0.02$ Hz	3
Nov. 23, 88	03H57M06.8S	5.4	Balapan	$1.8 (\pm 0.2) \times 10^{15}$	$0.70 \pm 0.02$ Hz	3
Dec. 17, 88	04H18M06.8S	5.9	Balapan	$1.3 (\pm 0.4) \times 10^{16}$	$0.52 \pm 0.03$ Hz	4
Jan. 22, 89	03H57M06.7S	6.0	Balapan	$1.2 (\pm 0.3) \times 10^{16}$	$0.60 \pm 0.04$ Hz	3
Feb. 12, 89	04H15M06.9S	5.8	Balapan	$9.5 (\pm 2.5) \times 10^{15}$	$0.59 \pm 0.03$ Hz	4
Jul. 8, 89	03H47M00.0S	5.6	Balapan	$3.5 (\pm 1.2) \times 10^{15}$	$0.70 \pm 0.05$ Hz	2
Sep. 2, 89	04H16M59.9S	5.1	Balapan	$8.2 (\pm 3.4) \times 10^{14}$	$1.01 \pm 0.07$ Hz	1
Oct. 19, 89	09H49M58.0S	5.9	Balapan	$1.0 (\pm 0.2) \times 10^{16}$	$0.64 \pm 0.04$ Hz	5
Aug. 16, 90	04H59M57.7S	6.2	Lop Nor	$7.9 (\pm 1.4) \times 10^{14}$	$0.54 \pm 0.02$ Hz	2
May 21, 92	04H59M57.5S	6.6	Lop Nor	$4.3 (\pm 0.7) \times 10^{16}$	$0.40 \pm 0.02$ Hz	4
Oct. 5, 93	03H59M57.6S	5.9	Lop Nor	$8.3 (\pm 0.2) \times 10^{15}$	$0.68 \pm 0.05$ Hz	7
Jun. 10, 94	06H25M58.0S‡	5.7‡	Lop Nor	$2.0 (\pm 0.4) \times 10^{15}$	$0.92 \pm 0.03$ Hz	5
Oct. 7, 94	03H25M58.0S‡	5.9‡	Lop Nor	$5.5 (\pm 0.2) \times 10^{15}$	$0.80 \pm 0.06$ Hz	8
May 5, 95	04H05M58.0S‡	5.9‡	Lop Nor	$7.8 (\pm 0.2) \times 10^{15}$	$0.66 \pm 0.04$ Hz	8

† The origin times, locations and magnitudes are from the ISC or PDE bulletin; the seismic moments and corner frequencies are obtained in this study using the explosion source model with  $\beta$  (equation (2)) set to be 0.75 (Poisson medium).

\* The Joint Verification Experiment (JVE) event.

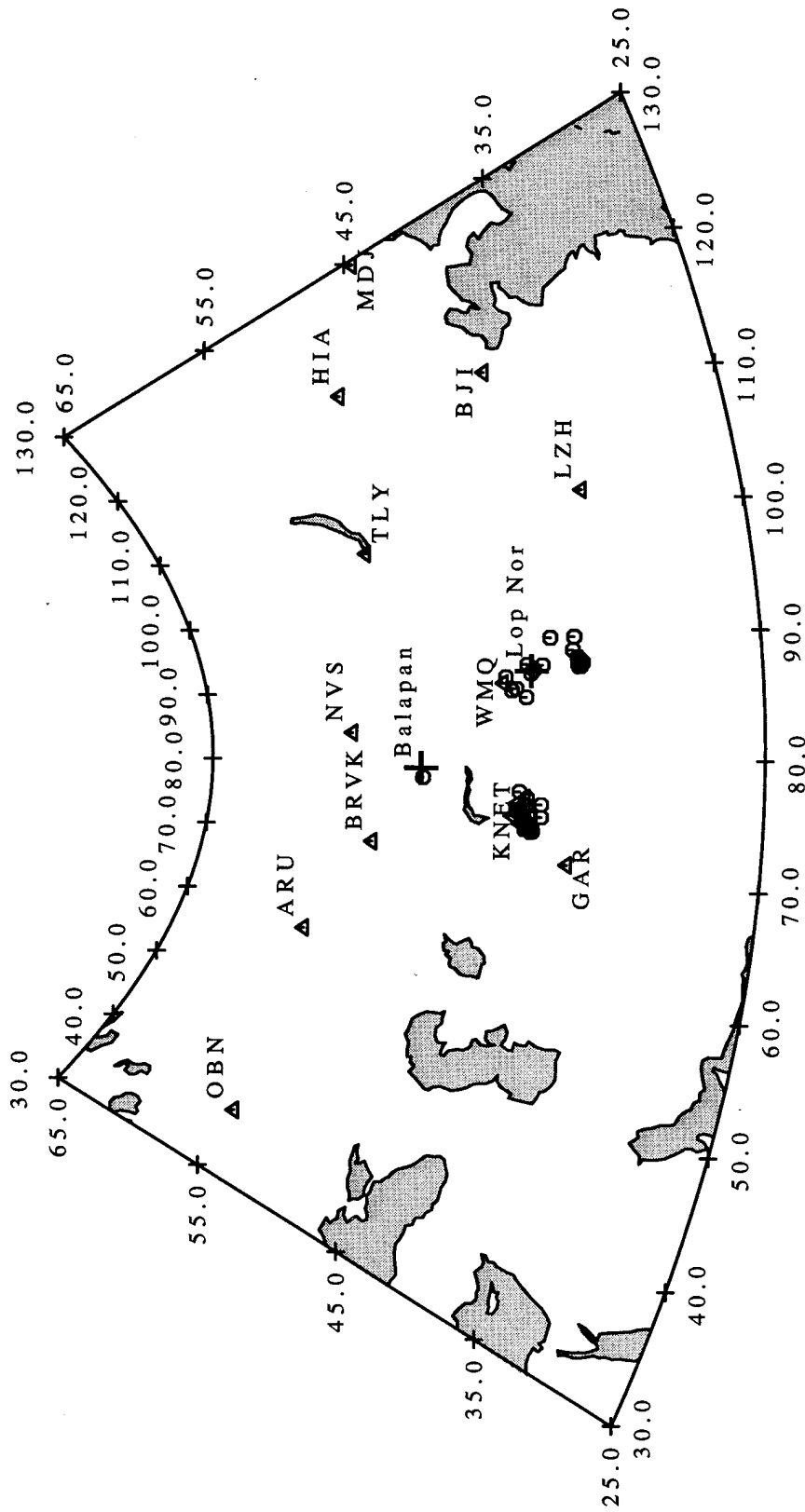
‡ USGS preliminary (PDE) estimate.

Table 2. Earthquakes Studied†

Number	Date	Origin Time h m s	Latitude (° N)	Longitude (° E)	$m_b$	$M_0$ (dyne-cm)	$f_c$ (Hz)	Number of Stations
1	03 Jan 88	20 09 21.4	38.431	91.340	4.4	$1.9 \times 10^{22}$	0.84	1
2	06 Feb 88	04 19 11.1	49.799	78.064	4.8	$7.0 \times 10^{21}$	0.65	1
3	15 Mar 88	15 55 24.3	42.210	75.509	4.5	$2.2 \times 10^{22}$	0.50	1
4	05 Mar 89	13 48 41.6	42.511	74.629	4.8	$7.0 \times 10^{22}$	0.60	1
5	14 Apr 89	22 57 59.6	41.132	74.525	4.6	$1.4 \times 10^{22}$	0.50	1
6	21 Jan 90	07 53 31.9	41.534	88.728	4.6	$1.0 \times 10^{22}$	0.80	1
7*	02 Feb 90	14 04 25.5	42.219	76.270	4.4	$1.4 \times 10^{22}$	0.76	2
8*	03 May 90	10 02 22.2	42.790	76.880	4.7	$3.8 \times 10^{22}$	0.70	3
9	19 Sep 90	08 05 57.3	38.001	88.940	4.4	$1.8 \times 10^{22}$	0.90	1
10*	03 Nov 90	17 25 13.8	40.882	89.071	5.1	$1.2 \times 10^{23}$	0.50	3
11	08 Jun 92	09 20 54.5	43.598	88.277	4.2	$5.0 \times 10^{21}$	1.00	1
12	10 Jun 92	02 37 01.2	38.623	90.147	4.4	$1.6 \times 10^{22}$	0.88	1
13*	19 Aug 92	10 17 35.2	42.265	73.252	5.1	$2.2 \times 10^{23}$	0.38	4
14	19 Aug 92	14 17 40.7	41.876	73.410	4.7	$6.1 \times 10^{22}$	0.42	1
15*	19 Aug 92	22 45 51.2	41.897	73.199	4.9	$6.0 \times 10^{22}$	0.60	2
16	20 Aug 92	01 28 02.5	41.751	73.361	4.6	$2.8 \times 10^{22}$	0.66	1
17	20 Aug 92	06 25 47.0	41.864	73.386	4.5	$3.2 \times 10^{22}$	0.63	1
18	20 Aug 92	06 52 41.8	41.951	73.215	4.1	$1.8 \times 10^{22}$	0.75	1
19	20 Aug 92	10 01 16.5	41.699	73.086	4.0	$1.8 \times 10^{22}$	0.70	1
20	20 Aug 92	12 22 47.3	41.991	73.377	4.8	$1.0 \times 10^{23}$	0.57	2
21	20 Aug 92	12 59 27.7	41.836	73.058	4.2	$1.9 \times 10^{22}$	0.88	1
22	20 Aug 92	16 30 45.4	41.837	73.633	4.2	$2.5 \times 10^{22}$	0.88	1
23	20 Aug 92	21 35 30.0	42.212	73.507	4.5	$1.2 \times 10^{22}$	0.87	1
24	21 Aug 92	04 14 32.7	41.923	73.503	4.7	$7.1 \times 10^{22}$	0.66	2
25	22 Aug 92	08 52 08.2	41.996	73.470	4.4	$2.3 \times 10^{22}$	0.76	1
26	23 Aug 92	00 28 06.2	41.950	73.746	4.1	$1.1 \times 10^{22}$	0.88	1
27	23 Aug 92	02 54 47.4	41.892	73.575	4.4	$1.7 \times 10^{22}$	0.77	1
28	23 Aug 92	07 15 07.3	41.909	73.463	4.7	$4.0 \times 10^{22}$	0.62	1
29	23 Aug 92	09 04 32.4	41.998	73.567	4.9	$8.5 \times 10^{22}$	0.70	2
30	23 Aug 92	20 11 42.4	41.951	73.447	4.4	$2.1 \times 10^{22}$	0.75	1
31	23 Aug 92	20 35 06.0	41.959	73.536	4.6	$5.1 \times 10^{22}$	0.61	1
32	26 Aug 92	07 40 36.7	41.785	73.387	4.8	$4.2 \times 10^{22}$	0.73	1
33	26 Aug 92	20 44 40.3	41.941	73.664	4.4	$1.0 \times 10^{22}$	0.66	1
34	26 Aug 92	22 01 15.0	41.928	73.552	4.6	$3.0 \times 10^{22}$	0.70	1
35	28 Aug 92	04 33 38.8	41.933	74.395	4.5	$1.1 \times 10^{22}$	0.69	1
36	25 Sep 92	07 59 59.9	41.763	88.387	5.0	$1.2 \times 10^{22}$	0.82	1
37	20 Oct 92	16 30 52.0	41.927	73.241	4.0	$7.0 \times 10^{21}$	1.08	1
38*	27 Nov 92	16 09 09.1	41.978	89.283	5.3	$1.4 \times 10^{23}$	0.48	3
39*	02 Feb 93	16 05 14.1	42.219	86.132	5.7	$3.7 \times 10^{23}$	0.34	4
40	17 Feb 93	02 00 25.8	38.321	89.484	5.1	$1.5 \times 10^{23}$	0.58	1
41	13 Apr 93	17 56 02.0	41.190	75.719	4.7	$1.1 \times 10^{23}$	0.46	1
42	14 Apr 93	08 31 09.7	42.904	87.045	4.4	$1.3 \times 10^{22}$	0.64	1
43	26 May 93	14 11 12.4	40.117	91.525	4.4	$8.0 \times 10^{21}$	0.82	2
44*	02 Oct 93	08 42 32.7	38.190	88.663	6.2	$4.8 \times 10^{24}$	0.21	7
45	02 Oct 93	09 20 12.2	38.206	89.284	4.9	$4.7 \times 10^{22}$	0.62	1
46*	02 Oct 93	09 43 19.5	38.169	88.605	5.8	$4.8 \times 10^{23}$	0.33	5
47*	02 Oct 93	17 23 33.3	38.171	88.690	5.6	$2.6 \times 10^{23}$	0.41	6
48	02 Oct 93	19 16 43.0	38.079	88.831	3.8	$7.4 \times 10^{21}$	1.10	1
49	02 Oct 93	23 49 59.7	38.359	88.878	4.8	$1.6 \times 10^{22}$	0.64	1
50	07 Oct 93	03 26 58.9	38.214	88.726	5.0	$3.4 \times 10^{22}$	0.68	2
51	12 Oct 93	20 49 23.4	38.276	88.604	4.7	$5.6 \times 10^{22}$	0.54	1
52	08 Jun 94	21 03 41.4	43.228	86.886	4.6	$1.2 \times 10^{22}$	0.69	1

† The origin times, locations and magnitudes are from the IRIS DMC; the seismic moments ( $M_0$ ) and corner frequencies ( $f_c$ ) are obtained in this study using the earthquake source model.

\* Events for which full inversion for  $M_0$ ,  $f_c$ ,  $Q$  and  $\eta$  for paths to station was performed. (for other events,  $Q$  was fixed at values determined along similar paths from earlier inversion).



**Fig. 1.** Locations of the 21 underground nuclear explosions (crosses), 52 earthquakes (circles) and 21 seismic stations (triangles) used in this study. Water covered areas are shaded. The numbers of stations providing Lg records are 17 for the explosions, and 11 for the earthquakes.

Station: CHM. Starting time=282.4sec. Dist=1157.8km

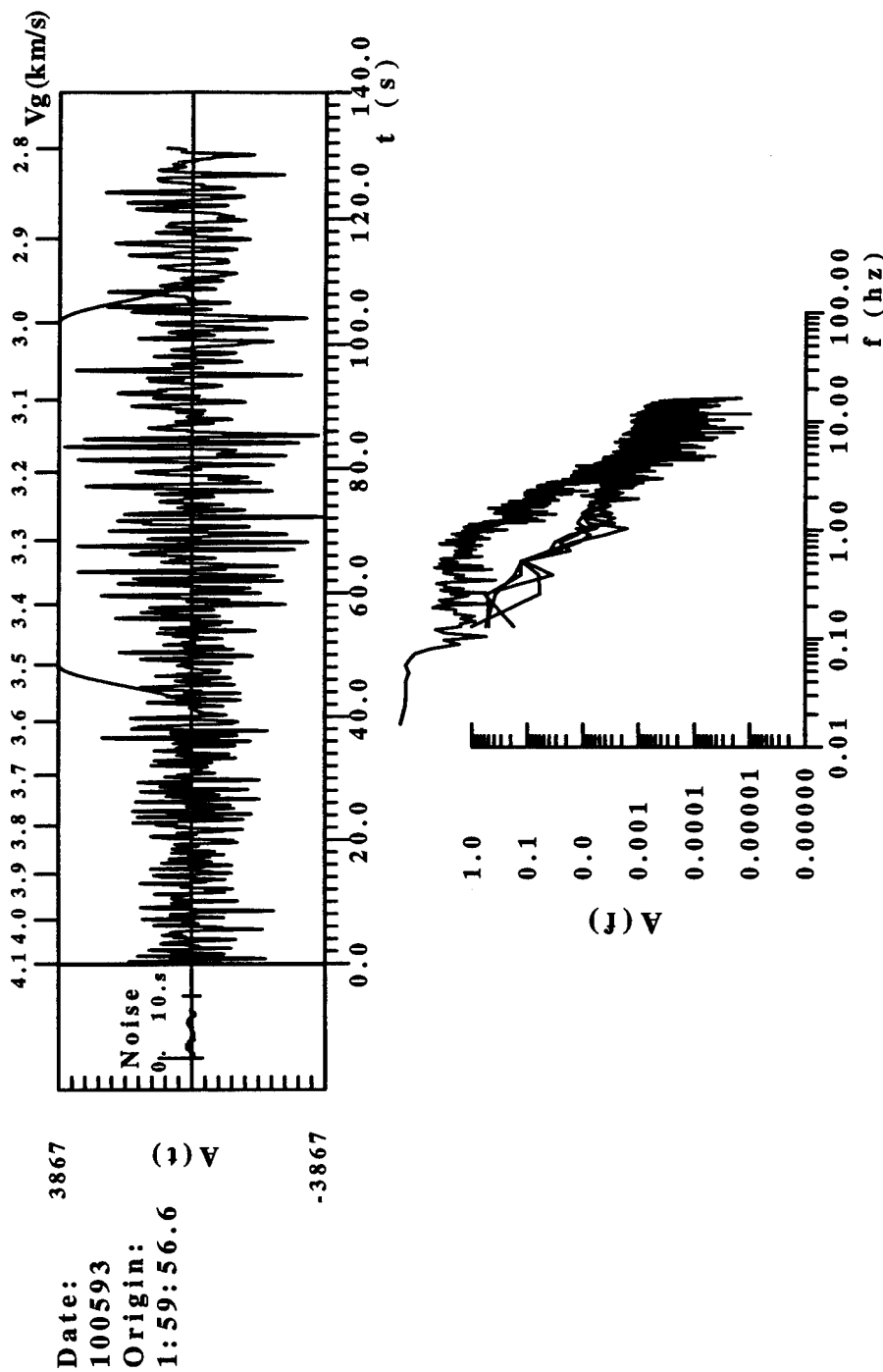


Fig. 2. (Top) Time series containing Lg from a Lop Nor explosion (see left of the panel) at KNET station CHM. Group velocities and time after the beginning of the window are indicated on the top and bottom of the panel. The smooth curve represents a 20 percent cosine window used in the analysis. (Bottom) The instrument-corrected Fourier amplitude spectra of Lg and noise prior to P.

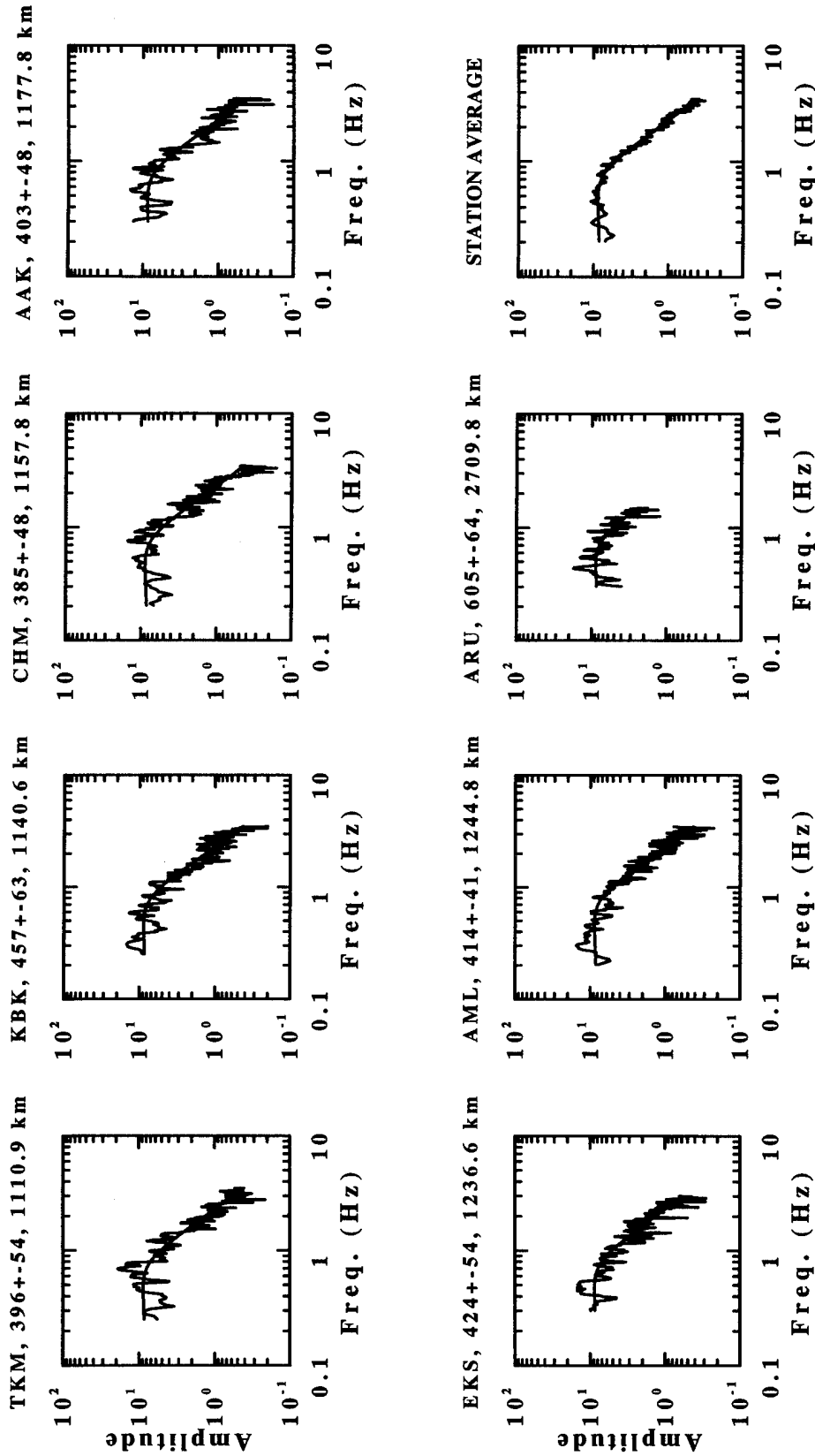
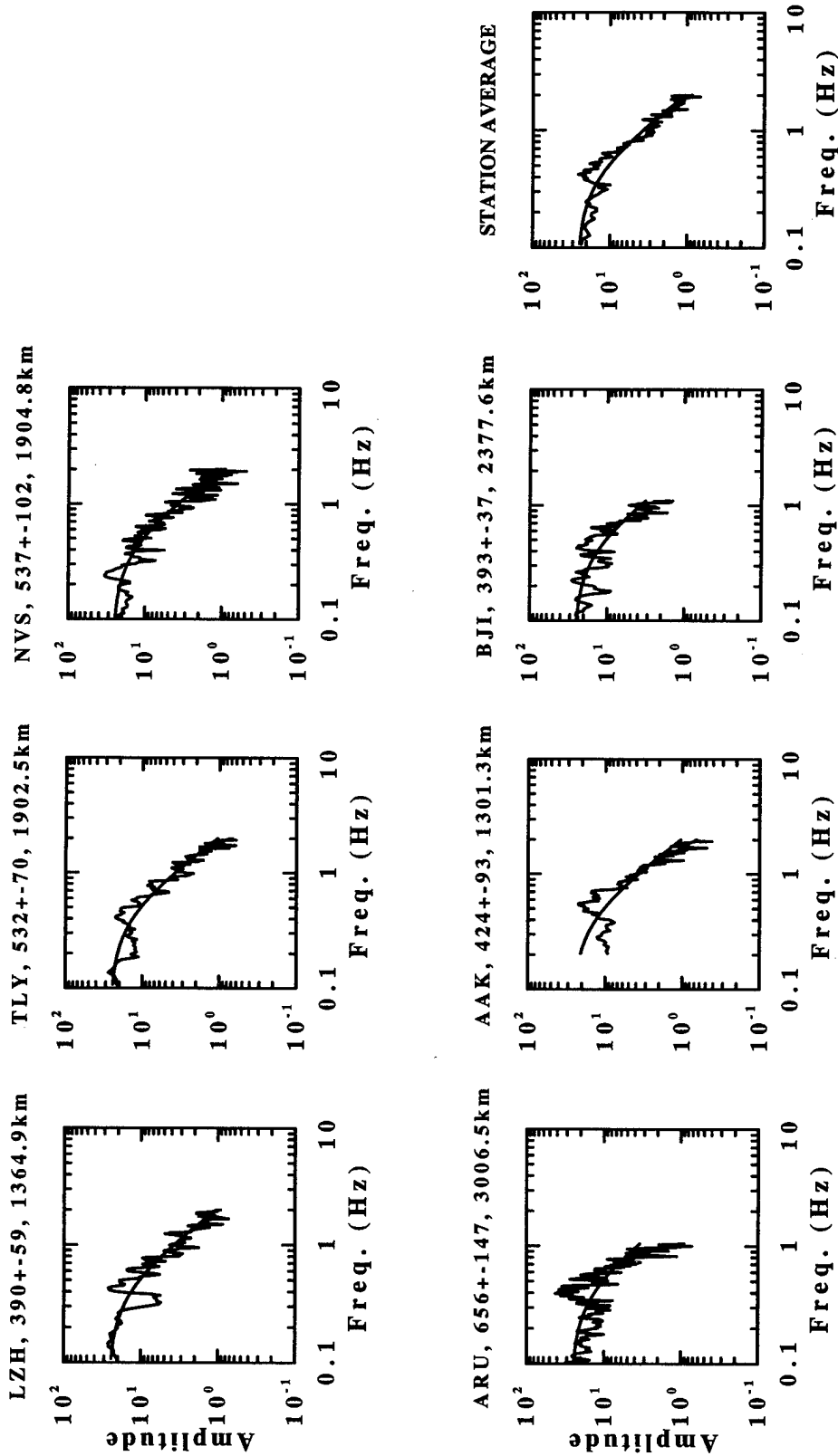
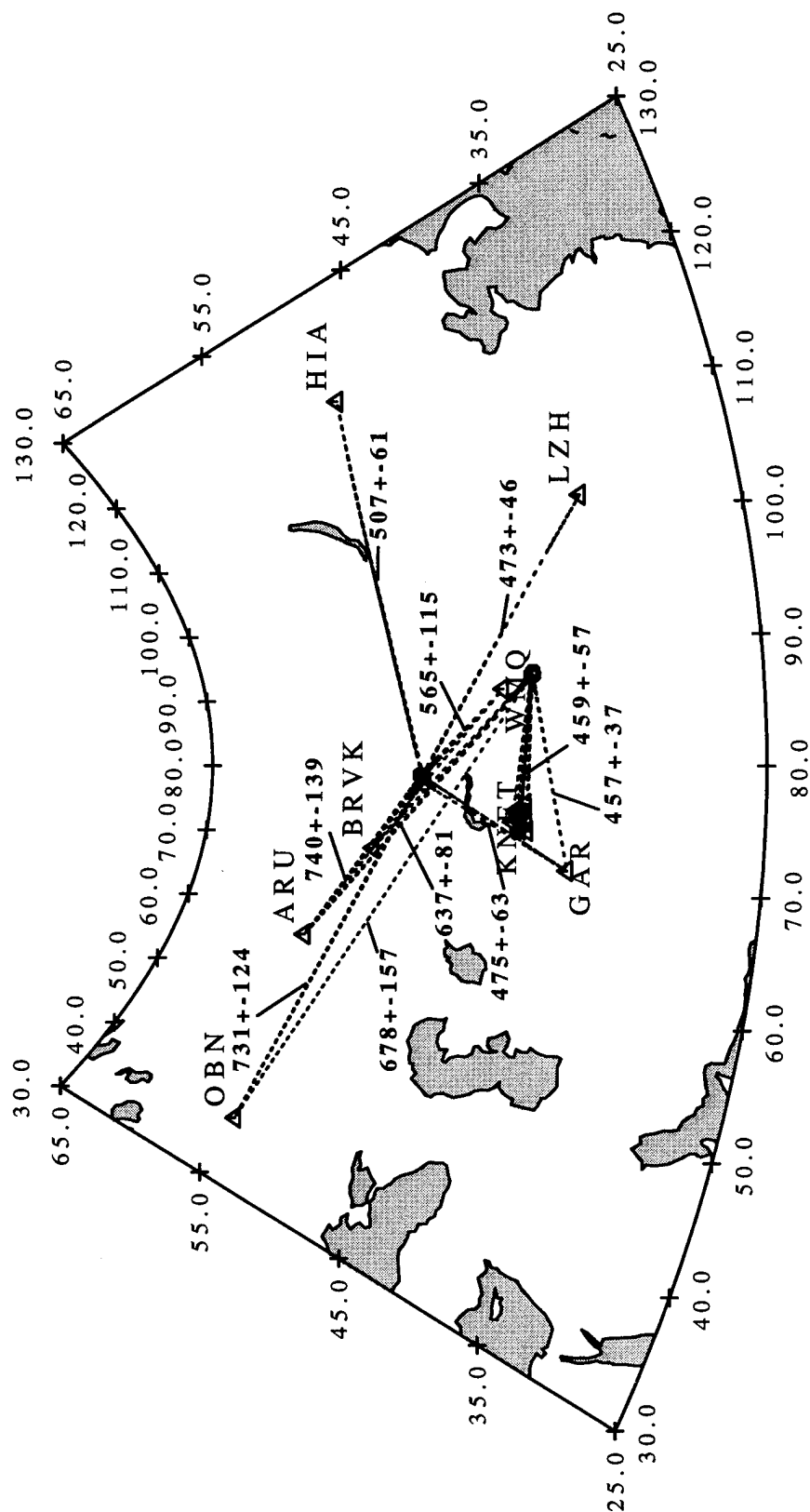


Fig. 3. Synthetic Lg source spectra for seven KNET and IRIS stations recording the October 5, 1993, Lop Nor explosion, versus the observed Lg spectra that are reduced to source by removing path effects. The lower right panel is the average for all of the seven stations. The synthetic spectra are calculated using optimal source spectral parameters ( $M_0 = 8.3 \times 10^{15}$  Nm,  $f_c = 0.68$  Hz) obtained in the inversion. Path  $Q_0$  values obtained in the inversion are written on the top of the panels, together with the epicentral distances.



**Fig. 4.** Synthetic Lg source spectra for six IRIS and CDSN stations recording the October 2, 1993, southern Xinjiang earthquake ( $M_b = 5.6$ ), versus the observed. The synthetic spectra are calculated using optimal source spectral parameters ( $M_0 = 2.6 \times 10^{16} \text{ Nm}$ ,  $f_c = 0.41 \text{ Hz}$ ) obtained in the inversion.



**Fig. 5 (a)** Lg  $Q_0$  values obtained for the great circle paths from the Lop Nor and Balapan test sites to the 17 IRIS, CDSN and KNET stations. Water-covered areas are shaded.

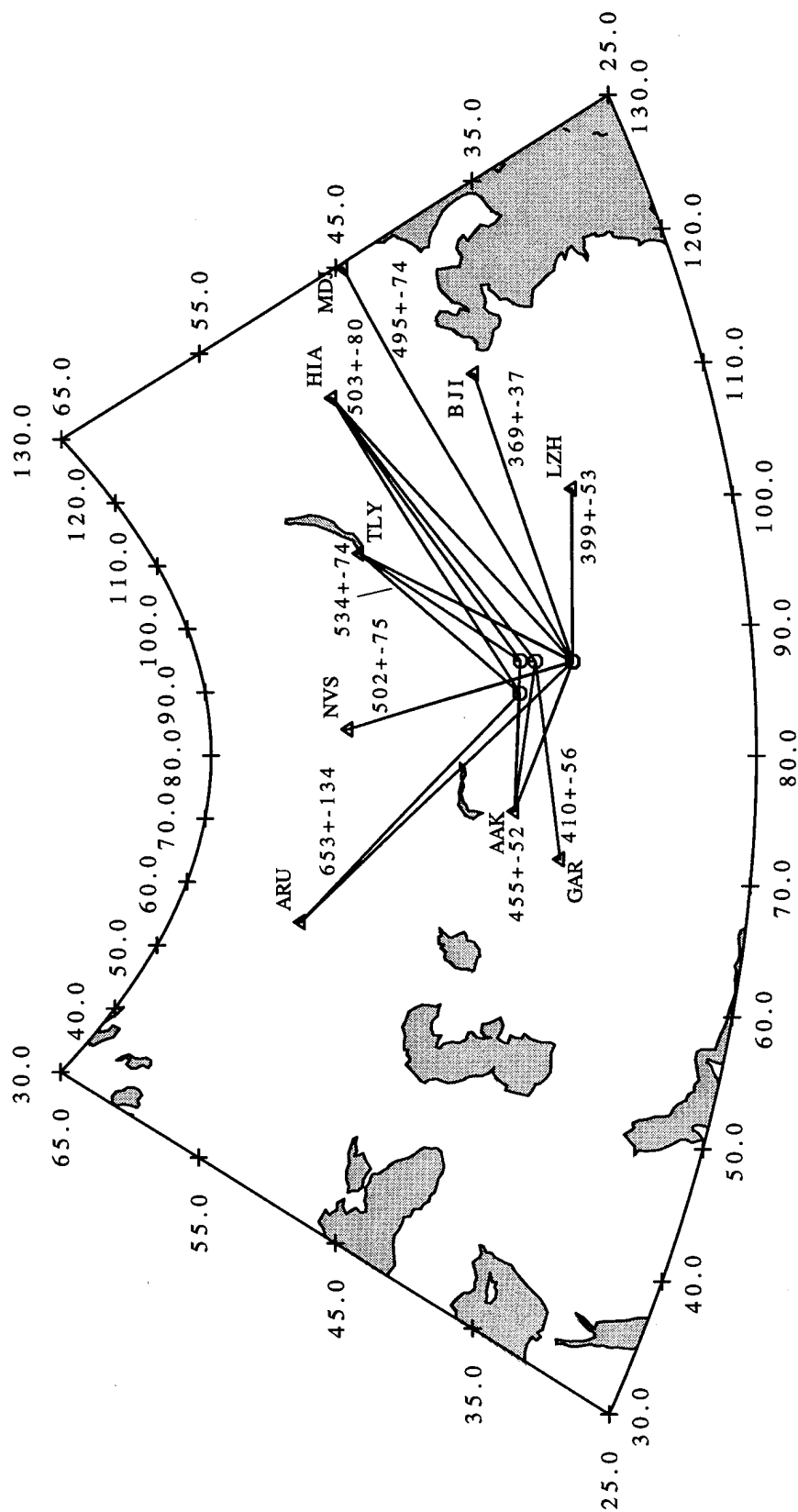


**Fig. 5(b)** Lg  $Q_0$  values obtained for the great circle paths from earthquakes in Xin Jiang, China to IRIS and CDSN stations.



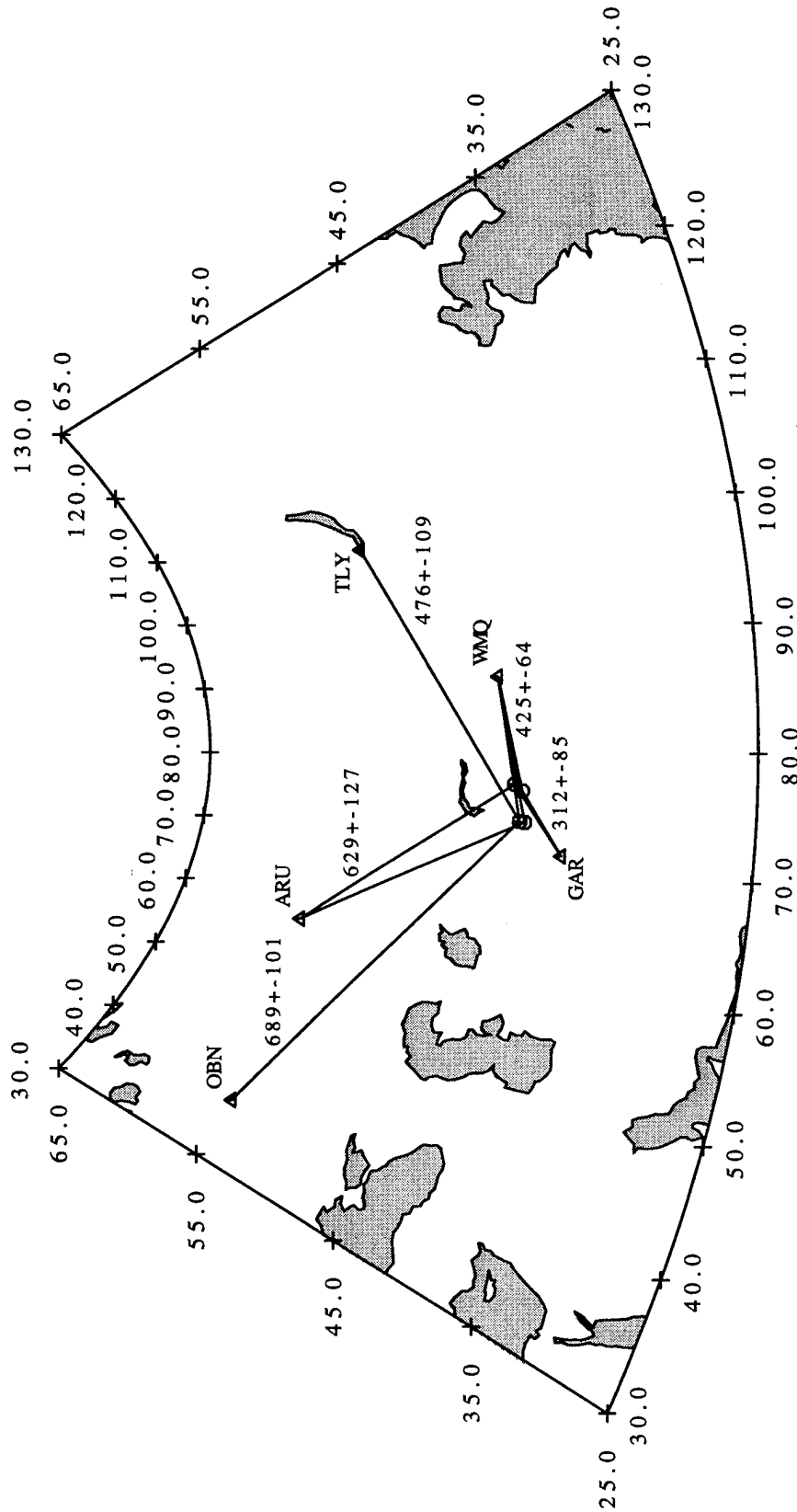
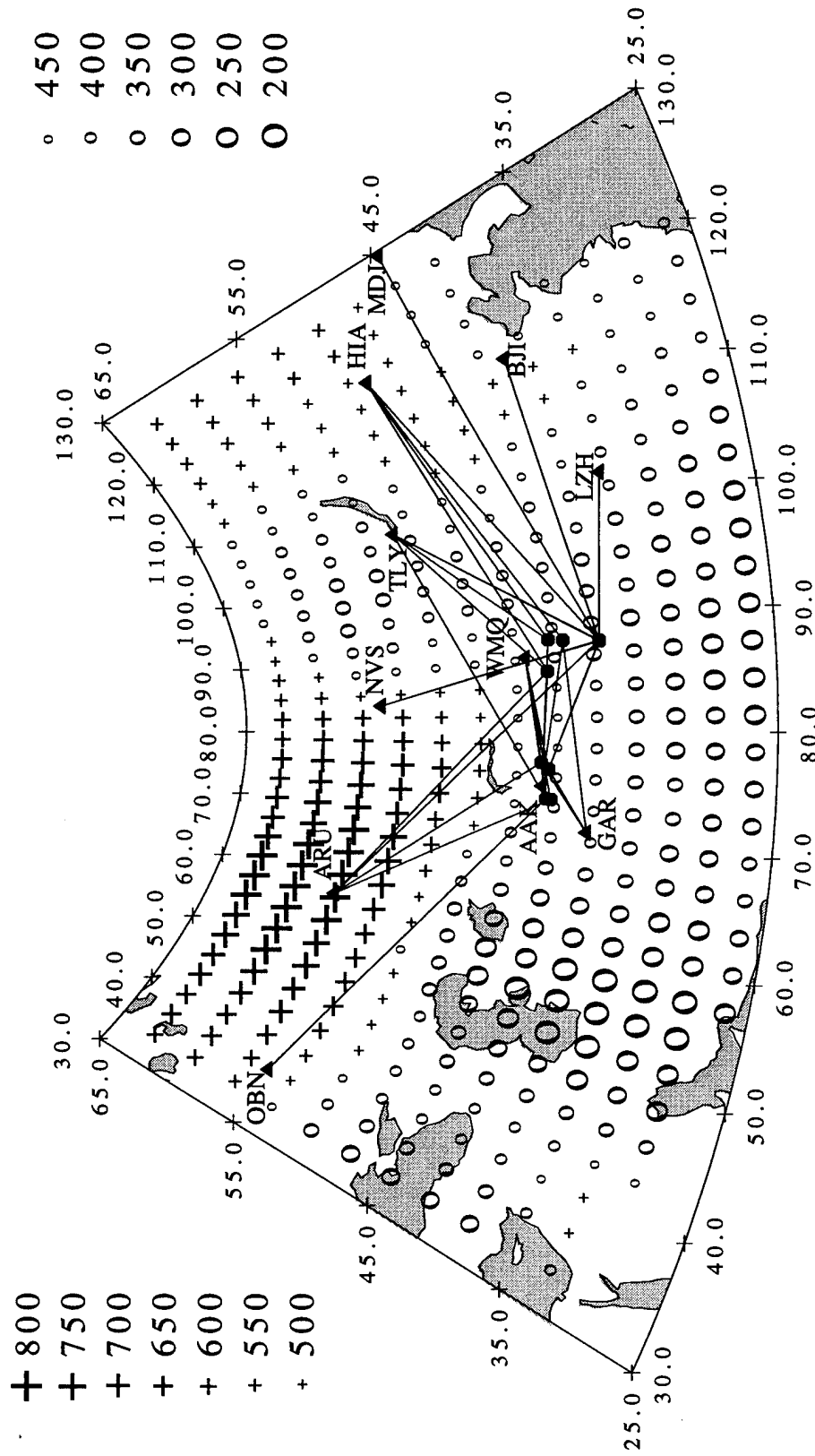


Fig. 5(c) Lg  $Q_0$  values obtained for the great circle paths from earthquakes in the central Asian Republics of the F.S.U. to IRIS and CDSN stations.



effects, resulting in reduced Lg spectra at the source. The fit between the observed Lg spectra (reduced to source) and the theoretical source spectrum for the explosion event (Figure 3) and that for the earthquake event (Figure 4) are both good, particularly for the station averages (lower right panels). The fit in Figure 3, though, appear to be better than that in Figure 4. This phenomenon is typical for all events studied, indicating a greater complexity in Lg source spectra of earthquakes than those of explosions in the study area.

#### **Agreements among 1 Hz Q measured using Lg from explosions, Lg from earthquakes and Lg coda**

In several previous studies (*eg.*, Kopnichev, 1977; Herrmann, 1980; Der *et al.*, 1984; Xie & Nuttli, 1988; Xie & Mitchell, 1990b; Ryaboy, 1990; Chun *et al.*, 1994), observed Lg coda Q values were similar to those of Lg Q when both were carefully measured. Considering the 3D complexity of the earth, however, the agreement between Lg Q and Lg coda Q is somewhat surprising. Regions where they do not agree are usually sites of major lateral crustal discontinuities; thus discrepancy between Lg Q and Lg coda Q maybe a tool to detect large-scale disruptions of the crustal waveguide (Xie & Mitchell, 1990b, Kennett *et al.*, 1991). In this study we have obtained Lg  $Q_0$  and  $\eta$  values for numerous paths covering a large area of central Eurasia. In Figures 5a through 5c we plotted the Lg  $Q_0$  values (Lg Q at 1 Hz) obtained for all of the path groups obtained in this study. To compare these Lg  $Q_0$  values with Lg coda  $Q_0$  values, in Figure 6 we plotted a portion of the tomographic Lg coda  $Q_0$  map by Xie & Mitchell (1991). The estimated errors of  $Q_0$  values in Fig. 6 are about 10% to 15%. Similarities in the  $Q_0$  values for each path in Figure 5a and those predicted for the same path in Fig. 6 are readily apparent. For example, from Lop Nor to the KNET stations, Fig. 5a gives an average  $Q_0$  of  $459 \pm 57$  whereas from Fig. 6 we can predict a  $Q_0$  around 450. From Lop Nor to stations ARU and OBN, Fig. 5a gives  $Q_0$  of  $637 \pm 81$  and  $678 \pm 157$ , respectively. These agree with corresponding predictions of around 650 and 700 based on Fig. 6. Agreement can also be found for paths from Balapan to various IRIS/CDSN stations. Xie (1993) has already discussed the latter agreement, using results from analyzing a much smaller data base. Since the explosion sources should have near-isotropic moment tensors, it is reasonable to assume that the source to Lg radiation does not vary significantly with azimuth. The agreement between the  $Q_0$  values in Figures 5a and 6 indicates, then, that the  $Q_0$  values obtained in this study using Lg from explosions have not been seriously biased by effects of large-scale 3D structural complications, such as the focusing/defocusing effects by the Tianshan mountain predicted by Bostock & Kennett (1990).

For earthquake sources, the possibility of non-isotropic source radiation pattern is expected to increase, and there is a concern that the  $Q$  measured using Lg from earthquakes may be biased by that radiation pattern. We note that the paths connecting the earthquakes near the Lop Nor test site and stations ARU, GAR and AAK in Figure 5b roughly overlap with the paths connecting the Lop Nor explosions and the respective stations in Figure 5a. For these three paths, Figure 5b shows  $Q_0$  values of  $653 \pm 134$  (to ARU),  $410 \pm 56$  (to GAR), and  $455 \pm 52$  (to AAK), respectively. These values agree, within the estimated uncertainties, with the corresponding values of  $637 \pm 81$ ,  $457 \pm 37$ , and  $459 \pm 57$  in Figure 5a. Therefore for all of the available overlapping paths, we find no difference between  $Q_0$  measured using Lg from earthquakes and  $Q_0$  measured using Lg from explosions.

For other paths in Figures 5b and 5c, no overlapping paths can be found in Figure 5a to warrant a comparison in  $Q_0$ , but we can still compare the Lg  $Q_0$  values for these paths with those predicted by the Lg coda  $Q_0$  map in Figure 6. In general, the  $Q_0$  values in Figures 5b and 5c are very compatible to those in Figure 6. For example, the Lg  $Q_0$  value along the path to station LZH in Figure 5b is  $399 \pm 53$ , which matches the values of about 350 to 400 in Figure 6. Similarities between  $Q_0$  values for other paths in Figures 5b or 5c and those in Figure 6 are readily apparent, indicating that the Lg  $Q_0$  measured using Lg from earthquakes are similar to those predicted by the Lg coda  $Q_0$  map.

We conclude that all comparisons available from this study indicate that the  $Q_0$  values measured using Lg from explosions agree with  $Q_0$  values measured using Lg from earthquakes, and these Lg  $Q_0$  values agree with previously mapped Lg coda  $Q_0$  values in the area. Although these agreements do not preclude possibilities of observing any future disagreement between Lg  $Q_0$  and Lg coda  $Q_0$ , it does indicate that the Lg  $Q_0$  values obtained in this study have not been seriously biased by effects of any non-isotropic source radiation patterns, or of any large-scale 3D structural complications, such as the focusing/defocusing effects by the Tianshan mountain predicted by Bostock & Kennett (1990).

#### **Comparison between Lg $\eta$ and Lg coda $\eta$**

We also compared the values of Lg  $\eta$ , the power-law frequency dependence of Lg  $Q$ , with the values predicted with an Lg coda  $\eta$  map (Xie and Mitchell, 1991). We found that when the epicentral distance ( $\Delta$ ) is less than about 2700 km, the Lg  $\eta$  obtained in this study agrees (within an uncertainty level of about 0.1 to 0.2) with the Lg coda  $\eta$ . At larger distances ( $\Delta > 2700$  km), the  $\eta$  values obtained in this study tend to be low (typically down to  $\sim 0.0$ ). This discrepancy may be caused by a number of reasons, including

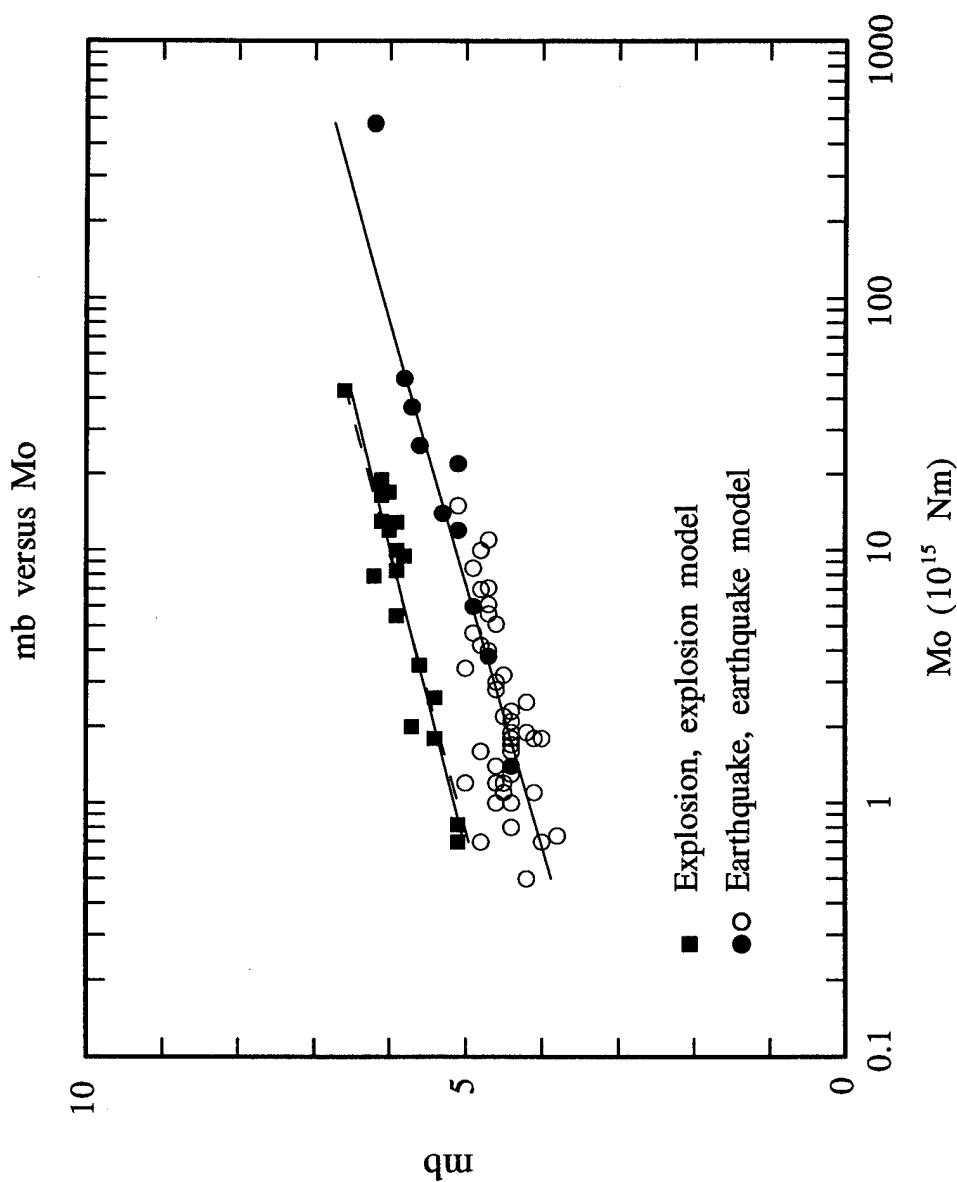


**Fig. 7.**  $M_b$  values versus logarithm of  $M_0$  values (in  $10^{15}$  Nm) obtained for explosions (squares) and earthquakes (circles). Solid circles represent values for earthquakes that are better recorded (*i.e.*, earthquakes with Lg recorded at three or more stations), and open circles represent values for earthquakes with Lg recorded at only one or two stations. Straight lines represent the linear regression fitting.

imprecisely estimated Lg  $\eta$  due to the narrower frequency bands, or effects of the earth's curvature at large  $\Delta$ . Other possible reasons for the discrepancy is being explored but can not be currently identified with confidence.

### Correlation between $M_0(\text{Lg})$ and ISC $M_b$

Figure 7 shows the  $M_0$  values obtained for the explosions (squares) and earthquakes (circles). The  $M_0$  values for the explosions are obtained with the explosion source model (equation (1)), and are the first ever obtained using Lg from underground nuclear explosions. We would therefore like to assess their reliability and consistency with the P wave seismic moments. For P waves the seismic moment,  $M_0^P$ , is related in theory to the displacement potential,  $\psi_\infty$ , via

$$\psi_\infty = \frac{M_0^P}{4\pi\rho\alpha^2} \quad , \quad (3)$$

where  $\rho$  and  $\alpha$  are the source-zone density and P wave velocity (Mueller, 1973; Aki *et al.*, 1974). Ringdal *et al.* (1992) obtained an empirical relationship between  $\psi_\infty$  and ISC body-wave magnitude,  $M_b$ :

$$\log \psi_\infty = 1.1M_b + -2.57 (+ - 0.11) \quad (4)$$

(equation (13) of Ringdal *et al.*, 1992). Substitute equation (3) into (4) we have

$$\log M_0^P = 1.1M_b - 2.57 - \log(4\pi\alpha^2) (+ - 0.11) \quad . \quad (5)$$

Assuming that  $\alpha = 5.2$  km/s and  $\rho = 2.7$  g/cm<sup>3</sup> (Li *et al.*, 1995), equation (3) becomes

$$\log M_0^P = 1.1M_b + 9.39 (+ - 0.11) \quad , \quad (6)$$

where  $M_0^P$  is in Nm. Equation (6) is empirical, and approximately relates the  $M_0^P$  to ISC  $M_b$ . To see if  $M_0^P$  predicted by equation (6) and the  $M_0$  derived for the explosions using Lg in this study are consistent, we plotted equation (6) in Figure 7 (dashed line). The agreement between  $M_0^P$  values predicted by equation (6) (dashed line) and the  $M_0$  values obtained in this study (in the  $M_b$  range between roughly 5.0 and 6.5) is very good. A linear regression over the Lg  $M_0$  and  $m_b$  values for the explosions in Fig. 7 yields

$$\log M_0 = 1.19(+ - 0.11) M_b + 8.85(+ - 0.64) \quad (7)$$

for  $M_0$  derived using Lg. The slope and intercept in (7) agrees with, within the uncertainties, those predicted by (6), even though the intercepts in both equations represent *extrapolations* of the linear trends to zero  $M_b$ .

Earlier observations have suggested that for explosions, the Lg magnitude (based on time domain amplitude measurement) correlated well with  $M_b$  (eg., Nuttli, 1986a, 1986b, 1988; Henson *et al.*, 1990; Ringdal *et al.*, 1992). These observations emphasize that both  $M_b$  and  $M_{bLg}$  are obtained by measuring short period ( $\sim 1$  Hz) amplitudes. The  $M_0$  values in this study, on the other hand, are obtained by treating Lg as multiple supercritically reflected S waves (Street *et al.*, 1975; Xie, 1993). Furthermore, the  $M_0$  values are mainly constrained by Lg spectra at lower frequencies (down to 0.1 to 0.2 Hz for the effective Lg pass-band). Thus the agreement between  $M_0^P$  and  $M_0$  obtained in this study suggests a consistency between the source size measured using multi-station average of short-period P amplitudes and that using longer period multiple supercritically reflected S waves.

The Lg  $M_0$  versus  $m_b$  for the 53 earthquakes in Figure 7 are subdivided into two groups: values represented by solid circles are for the earthquakes with Lg recorded at least three stations, whereas values represented by open circles are for the earthquakes that are recorded by only one or two stations. For the latter group of earthquakes, we typically only inverted the  $M_0$  and  $f_c$  values, with path  $Q_0$ ,  $\eta$  values fixed using *a priori* knowledge from other inversions. The solid line through the circles in Figure 7 represents a linear regression, which yields the following equation:

$$\log M_0 = 1.04(+ - 0.09) m_b + 10.66(+ - 0.52) \quad . \quad (8)$$

In Figure 7, the open circles show higher degree of deviation from the linear trend than shown by the solid circles; this is to be expected since the open circles correspond to events that are relatively poorly recorded.

When comparing the circles and squares in Figure 7, or equivalently, equations (7) and (8), the most important feature we find is that for the same  $M_0$  values, the  $m_b$  values from explosions tend to be systematically larger than those from the earthquakes. Physically, this means that at the same Lg moment level, the explosions tend to have higher body wave amplitudes around 1 Hz than the earthquakes.

### **Previously unresolved issues on the scaling between $M_0$ and $f_c$ values**

The nature of the scaling between  $M_0$  and  $f_c$  derived using the Lg source spectra have been controversial for quite a long time. For earthquake sources, an unresolved issue is whether the S to Lg transfer function is flat at the source. A flat transfer function was empirically proposed by Street *et al.* (1975) and was supported by numerical simulations using flat layered structures by Herrmann & Kijko (1983) and by Campillo *et al.* (1985). Several other authors (eg., Harr *et al.*, 1984, 1986; Mueller & Cranswick, 1985) however, disagree with the idea of a flat transfer function, based on the interpretation of

observational results. They argued that corner frequencies ( $f_c$ ) estimated using Lg from many intra-plate earthquakes in North America are systematically lower than the  $f_c$  values estimated using local S waves from the same earthquakes. Mueller & Cranswick (1985) suggested that the  $M_0$  values estimated using local S waves scaled with  $f_c^{-3}$ , whereas  $M_0$  values estimated using the Lg wave scaled with  $f_c^{-4}$ . They further suggested that  $f_c$  estimated using any regional phases may be biased. Before this study, it seemed unclear to us whether the proposed systematically lower  $f_c$  values obtained using Lg were caused by the use of imprecise, path-invariant  $Q_{Lg}$  values, or caused by some inherent difference between the excitations of Lg and S waves by sources in realistic 3D media.

Sereno *et al.* (1988), during a novel simultaneous inversion of source spectra and Q using both Lg and Pn waves, assumed path-invariant Q and a scaling of  $M_0 \sim f_c^{-3}$  for Pn and Lg excited by both explosions and earthquakes. That scaling disagrees with those proposed by Harr *et al.* (1984, 1986) and Mueller & Cranswick (1985) when earthquakes are concerned. Sereno *et al.* obtained several important and interesting results in their study. One intriguing possibility found in their work is that in terms of seismic moment, the Lg excitation efficiency by explosions appears to be lower by a factor of 0.27 than that by earthquakes. While that result is interesting, we feel that it may have been affected by the various assumptions made, as cautioned by the authors. It would be very interesting to see whether one could obtain the same result without some of the assumptions by Sereno *et al.*

In view of the previous debates/unresolved issues on the Lg excitation, much of this study has been directed to further explore the answers to three fundamental questions in the excitation of the Lg by various seismic sources, summarized in the following:

- (1) Which scaling relation, *i.e.*,  $M_0 \sim f_c^{-3}$  or  $M_0 \sim f_c^{-4}$ , is a better representation of Lg excitation by seismic sources?
- (2) Is the transfer function between local S and Lg flat?
- (3) Is there any fundamental difference between Lg excitation by explosions and by earthquakes?

### Scaling between $M_0$ and $f_c$ values for explosions

The method used in this study (see the beginning of section II) allows us to explore the answers to the questions in the last section without making any *a priori* assumptions of path-invariant Lg Q, or of the scaling between  $M_0$  and  $f_c$ . In Figure 8, we plotted the Lg  $M_0$  and  $f_c$  for explosion sources, obtained using the explosion source model (equation (1)). The correlation between the logarithm of  $M_0$  and  $f_c$  values in Figure 8 is linear and



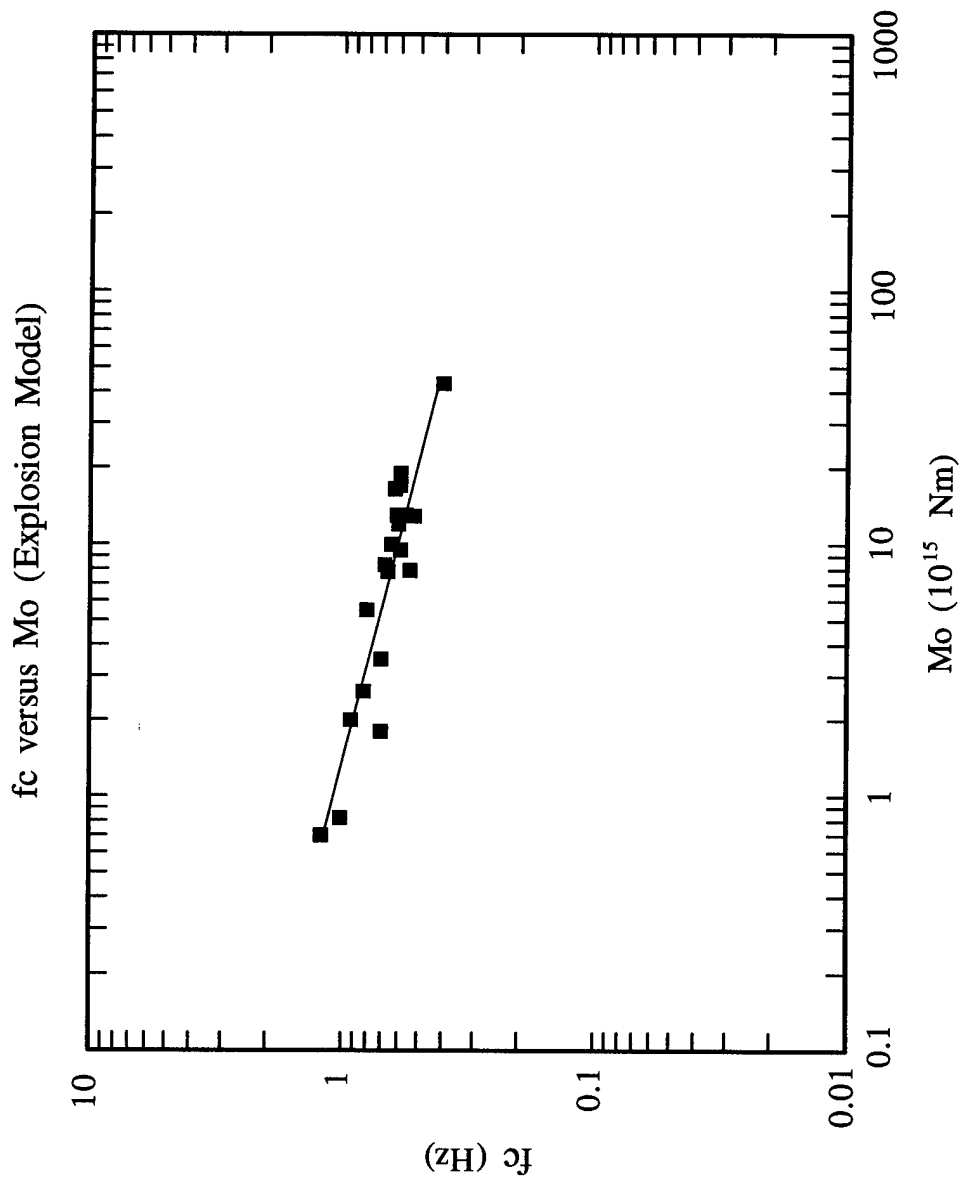


**Fig. 8.** Logarithm of  $M_0$  (in  $10^{15}$  Nm) versus logarithm of  $f_c$  values for the explosions studied, obtained by inverting the Lg spectra using the explosion source model. Straight line represents the linear regression fitting.

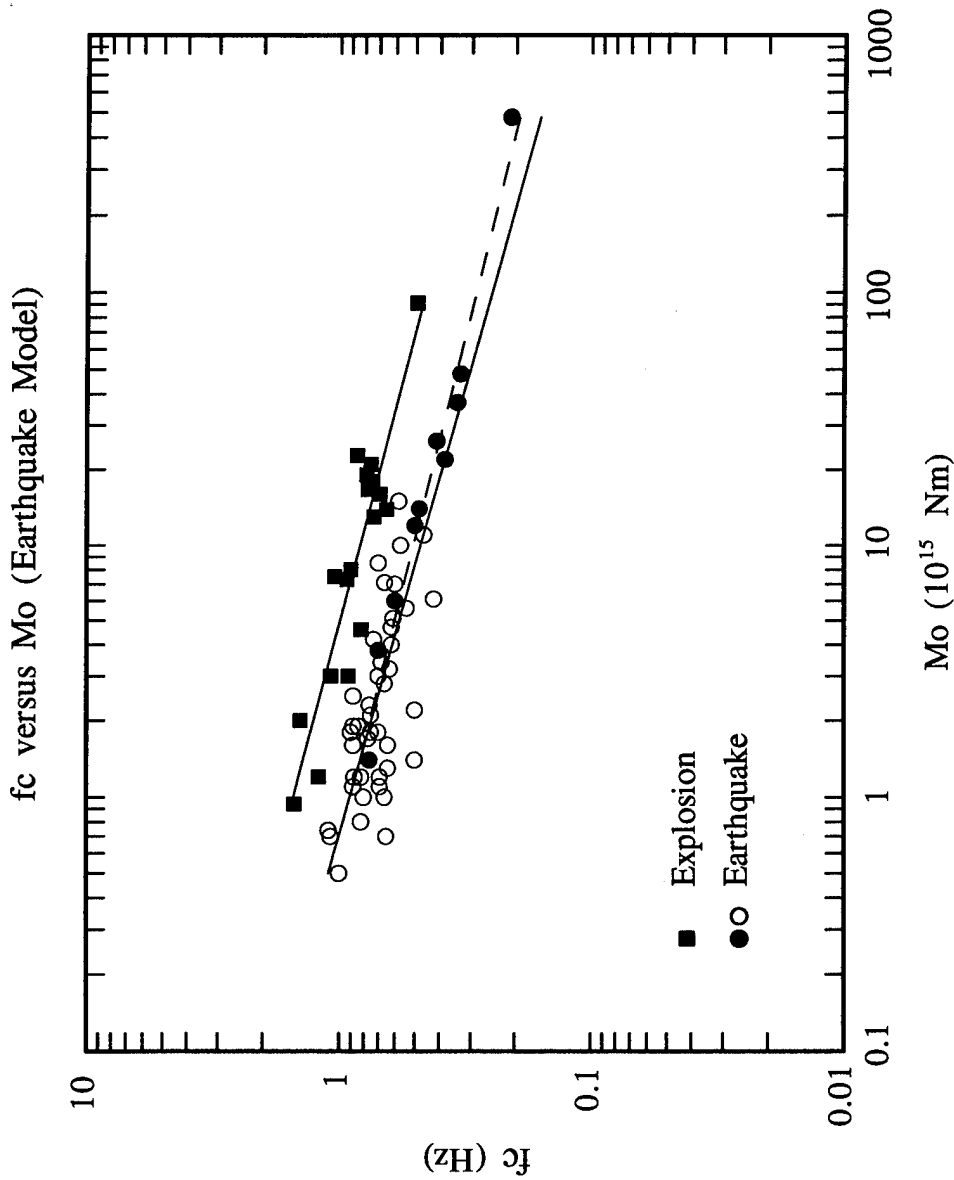


**Fig. 9.** Logarithm of  $M_0$  versus logarithm of  $f_c$  values for the earthquakes and explosions studied, all obtained by using the earthquake source model. Solid circle represent values for earthquakes with Lg recorded at multiple ( $\geq 3$ ) stations, and open circles represent the values for earthquakes with Lg recorded by fewer stations. Squares represent values for explosions, obtained using the earthquake source model. The two solid lines represent the linear regressions over all earthquakes and all explosions, respectively. The dashed line represent the linear regression over the solid circles only.

a regression analysis yields the following relationship:

$$\log M_0 = 15.12(\pm 0.22) - 3.98(\pm 0.43) \log f_c, \quad (9)$$

which suggests an  $M_0 \sim f_c^{-4}$  scaling.

### Scaling between $M_0$ and $f_c$ values for earthquakes

Figure 9 shows the Lg  $M_0$  and  $f_c$  values for the earthquake sources, obtained using the earthquake source model (equation (2)). Again, solid circles represent values for earthquakes with Lg recorded by multiple ( $\geq 3$ ) stations, and open circles represent earthquakes with Lg recorded by only one or two stations. A linear regression over all of the 52 circles yields

$$\log M_0 = 14.85(\pm 0.30) - 3.56(\pm 0.30) \log f_c \quad (10)$$

(solid line in Figure 9). If only solid circles (earthquakes with multiple Lg records) in Figure 9 are used, a linear regression yields

$$\log M_0 = 14.81(\pm 0.16) - 4.04(\pm 0.25) \log f_c \quad (11)$$

(dashed line in Figure 9). The slopes and intercepts in (10) and (11) overlap within the estimated uncertainty, with uncertainties (11) being smaller, probably due to that the corresponding Lg  $M_0$  and  $f_c$  values are better constrained when multiple records are available. Both equations suggest that  $M_0$  scale with  $f_c^{-\alpha}$ , with  $\alpha$  being closer to 4 than to 3.

### Dependence of $M_0$ , $f_c$ estimates on theoretical source models

A comparison between the  $M_0$  -  $f_c$  scaling derived for the explosions using the explosion source model (Figure 8; equation (9)) with those for the earthquakes using the earthquake model (equations (10) and (11)) will not be useful for the purpose of explosion discrimination since in deriving equation (9), we knew *prior* to the inversions that the events were explosions and accordingly, we have used the explosion source model in the inversions. For the purpose of future discrimination of explosions from earthquakes, it is desirable to simulate a situation when we do not know that the explosions under study are explosions, and treat them as earthquakes in the inversion. Therefore for the 21 explosions, we conducted inversions using the earthquake source model with no overshoot (equation (2) in section II). The resulting  $M_0$  and  $f_c$  values are plotted in Figure 9 as squares. A linear regression over these values yields the following relation:

$$\log M_0 = 15.69(\pm 0.23) - 3.83(\pm 0.45) \log f_c. \quad (12)$$

The slope in equation (12) suggests that the scaling of  $M_0 \sim f_c^{-4}$  is roughly preserved, even

though an earthquake source model is used in the inversion. On the other hand, the intercept predicted by equation (12) differs from that predicted by (9) by  $0.57 (\pm 0.45)$ . This means that the  $M_0$  values obtained with the explosion source model are systematically lower by a factor of 0.27 than those obtained with the earthquake source model. This factor coincides with the  $\kappa$  value of 0.27 obtained by Sereno et al. (1988), who studied *different sources (earthquakes and explosion) with the same (explosion) source model*, and proposed that the low  $\kappa$  value indicates a depletion of Lg by explosions. In this study, however, both (12) and (9) are obtained using the same explosion data set, and the factor of 0.27 must have arisen solely because of the model-dependence of the inversion, rather than any fundamental difference between the excitation of Lg by different source types. Physically, this model-dependence is due to the effect of overshoot in the explosion source model (equation (1)), which tends to downsize the seismic moment and/or corner frequency with an observed Lg spectrum. This model dependence makes it more obvious that for the purpose of future explosion discrimination, it is desirable to compare the  $M_0 - f_c$  scaling for the explosions with the corresponding scaling for the earthquakes, both derived using the same (preferably earthquake) source model, to look for any systematic differences. In the next section we present such a comparison using results obtained in this study.

### **Comparison between $M_0 - f_c$ scalings for earthquakes and explosions**

As mentioned in the above sections, the circles and squares Figure 9 represent  $M_0$  and  $f_c$  values estimated by applying the same (earthquake) source model to earthquakes and explosions, respectively. It is obvious that the distributions of circles and squares in Figure 9 show systematically different trends. At any fixed  $M_0$  level,  $f_c$  values for explosions (squares) are systematically higher than those for earthquakes (circles). Consequently, the corresponding linear regression fittings in equations (12) and (10) (or (11)) differ in their intercept by about 0.9, despite that the slopes are all similar (close to -4.0). Physically, this phenomenon means that the Lg excitation by explosions tend to be enriched in high frequency contents, as compared to Lg by earthquakes. We may use this phenomenon to form a basis for discriminanting explosions from earthquakes, but there are two complications associated with this potential discriminant. The first is that some open circles in Figure 9 overlap with the squares, but all of the filled circles are unambiguously separated from the squares. This suggests that a discriminant of explosion using the  $M_0 - f_c$  scalings should be used with caution when there are only one or two stations recording the Lg from an seismic event, either due to a sparse-station coverage or a small event size. The second complication is that the phenomenon of an enriched high

frequency Lg excitation by the explosions, observed in this study for the Lop Nor and Balapan Test Sites, appears to be opposite to what was observed for the Nevada Test Site (e.g., Murphy and Bennett, 1982; Bennett and Murphy, 1986; Walter *et al.*, 1995). This suggests that there may be some significant variations in the detailed mechanism of excitation of Lg by explosions with varying tectonic/geological environments, and any discriminant using Lg developed for one test site may not be directly transportable to another test site.

### **Implications on the difference between excitations of local S and Lg**

It has been generally believed that the  $M_0$  and  $f_c$  values of earthquakes, estimated using local S waves, tend to scale as  $M_0 \sim f_c^{-3}$  (pages 19 and 20). The fact that equations (10) and (11) both suggest slopes that are closer to -4 than -3 suggests that the Lg  $M_0 - f_c$  scaling differs from the corresponding scaling derived using local S waves. This probable difference has a profound implication in the mechanism of Lg excitation. The implication, however, is not as direct as desired. A systematic difference between the excitation of local S and Lg waves should be confirmed with more direct comparisons of spectra of S and Lg from the same events.

## **IV. FUTURE RESEARCH**

Based on the results of this study, we recommend that future research be conducted in the following areas:

- (1) Establish more precise, perhaps distance and frequency dependent geometrical spreading for the Lg phase and other regional phases based more substantial observations, made with more data, and synthetics using more realistic velocity structures.
- (2) Explore why the Lg excitation by explosions in different test sites vary in levels of high-frequency contents relative to low-frequency contents.
- (3) Compare frequency content of Lg with that of S waves observed at smaller distances (e.g., the Sg wave), and further explore if and why the local S waves exhibit a different  $M_0 - f_c$  scaling than the Lg wave.
- (4) Apply the same methodology in this study to the spectral characteristics of excitation and propagation of other regional phases, particularly the Pg and Pn phases, and systematically evaluate the P/Lg spectral ratio discriminant. Also, test to see if the

P/Lg discriminant is more reliable than the Lg discriminant.

## V. REFERENCES

- Aki, K., M. Bouchon & P. Reasenberg, 1974. Seismic source function for an underground nuclear explosion, *Bull. Seism. Soc. Am.*, **64**, 131-148.
- Bennett, T.J. and R. Murphy, 1986. Analysis of seismic discrimination capabilities using regional data from western United States events, *Bull. Seism. Soc. Am.*, **76**, 1069-1086.
- Bostock, M.G. & B.L.N. Kennett, 1990. Effect of 3-D structure on Lg propagation patterns, *Geophys. J. Int.*, **101**, 355-365.
- Campillo, M., J. Plantet and M. Bouchon, 1985. Frequency-dependent attenuation in the crust beneath central France from Lg waves: data analysis and numerical modeling, *Bull. Seism. Soc. Am.*, **75**, 1395-1411.
- Chun, Y.P., J. Liu, T. Zhu & X.R. Shih, 1994. Abnormal Lg coda Q in Beijing area, *Geophys. Res. Lett.*, **21**, 317-320.
- Harr, L. C., Fletcher, J.B., & Mueller, C.S., 1984. The 1982 Enola, Arkansas, swarm and scaling of ground motion in eastern United States, *Bull. Seism. Soc. Am.*, **74**, 2463-2482.
- Harr, L. C., Mueller, C.S., Fletcher, J.B., & Boore, D.M., 1986. Comments on "Some recent Lg phase displacement spectral densities and their implications with respect to prediction of ground motions in Eastern North America" by R. Street, *Bull. Seism. Soc. Am.*, **76**, 291-295.
- Henson, R.A., F. Ringdal, and P.G. Richards, 1990. The stability of RMS Lg measurements and their potential for accurate estimation of the yields of Soviet underground nuclear explosions, *Bull. Seism. Soc. Am.*, **80**, 2106-2126.
- Herrmann, R.B. and A. Kijko, 1983. Modeling some empirical Lg relations, *Bull. Seism.*

*Soc. Am.*, **56**, 157-172.

Kennett, B.L.N., M.G. Bostock and J.K. Xie, 1990. Guided wave tracking in 3D-a tool for interpreting complex regional seismograms., *Bull. Seism. Soc. Am.*, **80**, 633-642.

Li, Y., Toksoz, N.M. & W. Rodi, 1995. Source time functions of unclear explosions and earthquakes in Central Asia determined using empirical Green's functions, *J. Geophys. Res.*, **100**, 659-674.

Mueller, G., 1973. Seismic moment and long period radiation of underground nuclear explosions, *Bull. Seism. Soc. Am.*, **63**, 847-857.

Mueller, C.S. & Cranswick, E., 1985. Source parameters from locally recorded aftershocks of the 9 January 1982 Miramichi, New Brunswick, earthquake, *Bull. Seism. Soc. Am.*, **75**, 337-360.

Murphy, J.R. and Bennett, T.J., 1982. A discrimination analysis of short-period regional seismic data recorded at Tonto Forest Observatory, *Bull. Seism. Soc. Am.*, **72**, 1351-1366.

Nuttli, O.W., 1986a. Yield estimates of Nevada Test Site explosions obtained from seismic Lg waves, *J. Geophys. Res.*, **91**, 2737-2151.

Nuttli, O.W., 1986b. Lg magnitudes of selected East Kazakhstan underground explosions, *Bull. Seism. Soc. Am.*, **76**, 1241-1251.

Nuttli, O.W., 1988. Lg magnitudes and yield estimates for underground Novaya Zemlya nuclear explosions, *Bull. Seism. Soc. Am.*, **78**, 873-884.

Pan, Y., Mitchell, B.J. & Xie, J., 1992. Lg coda Q across Northern Eurasia, paper presented at the 14th annual PL/DARPA research symposium, September 1992.

Ringdal, F., Marshall, P.D. & R.W. Alewine, 1992. Seismic yield determination of Soviet underground explosions at the Shagan River test site, *Geophys. J. Int.*, **109**, 65-77.

- Ryaboy, V.Z., 1990. Earth crust and upper mantle Q-structure beneath northern Eurasia, (abs), *Seismo. Res. Lett.*, **62**, 32.
- Sereno, T.J. & J. Given, 1990. Pn attenuation for a spherically symmetric Earth model, *Geophys. Res. Lett.*, **17**, 1141-1144. 2089-2105.
- Street, R.L., R.B. Herrmann and O.W. Nuttli, 1975. Spectral characteristics of the Lg wave generated by central United States earthquakes, *Geophys. J. R. Astr. Soc.*, **41**, 51-63.
- Street, R.L., 1984. Some recent Lg phase displacement densities and their implications with respect to the prediction of ground motion in Eastern North America, *Bull. Seism. Soc. Am.*, **74**, 757-762.
- Vernon, F.V., 1991. Kyrghizstan seismic telemetry network, *IRIS Newsletter*, **XI**, No. 1, 7-9.
- Walters, W.R., K.M. Mayeda and H.J. Patton, 1995. Phase and spectral ratio discrimination between NTS earthquakes and explosions. Part I: Empirical observations, *Bull. Seism. Soc. Am.*, **85**, 1050-1067.
- Xie, J. and B.J. Mitchell, 1990a. A back projection method for imaging large scale lateral variation in Lg coda Q with application to continental Africa. *Geophysical Journal*, **100**, 161-181.
- Xie, J. & Mitchell, B.J. 1990b. Attenuation of multiphase surface waves in the Basin and Range Province, part I: Lg and Lg coda, *Geophys. J. Int.*, **102**, 121-137.
- Xie, J. and B.J. Mitchell B.J. 1991. Lg coda Q across Eurasia, in *Yield and discrimination studies in stable continental regions*, B.J. Mitchell (ed). Report PL-TR-91-2286, Phillips Laboratory, Hanscom Air Force Base, MA, 77-91.
- Xie, J. 1993. Simultaneous inversion of source spectra and path Q using Lg with applications to three Semipalatinsk explosions, *Bull. Seism. Soc. Am.*, **83**, 1547-1562.



## VI. PUBLICATIONS

Mitchell, B.J. & J. Xie, 1994. Attenuation of multiphase surface waves in the Basin and Range Province-III. Inversion for crustal anelasticity, *Geophys. J. Int.*, **116**, 468-484.

Xie, J., Cong, L. & B.J. Mitchell, 1996. Spectral characteristics of Lg excitation by underground nuclear explosions in Central Asia, *J. Geophys. Res.*, in press.

Cong, L., J. Xie & B.J. Mitchell, 1996. Characteristics of the excitation and propagation of Lg from earthquakes in Central Asia, in preparation.

Ni, J., Herrmann, R.B. & B.J. Mitchell, 1996. A student's note on radiation patterns for moment tensor sources, submitted to *Seism. Res. Lett.*.

## VII. PROFESSIONAL PERSONNEL

Investigators involved in the two-year research include Dr. Jiakang Xie (the P.I.), Dr. Brian J. Mitchell (the co-P.I.), and Mr. Lianli Cong (a graduate student).

## VIII. PAPERS PRESENTED AT MEETINGS

Mitchell, B.J., Pan, Y., Chen, D. & J-K. Xie, 1993. Q and crustal evolution in stable continental regions, (*Abs*), *Seism. Res. Lett.*, **64**, 262.

Xie, J., Cong, L. & B.J. Mitchell, 1994. Source spectral scaling and depth determination from Lg spectra, in *Papers presented at 16th Annual PL/DARPA Seismic Research Symposium*, 386-392, 7-9 Sep. 1994, Thornwood Conference center, Thornwood, New York.

Xie, J. L. Cong and B.J. Mitchell, 1994. Relationship between seismic moment and corner frequency estimated using Lg from underground nuclear explosions, *EOS, Trans. AGU, 1994 Fall Meeting*, **75**, 477.

Cong, L., Xie, J. and B.J. Mitchell, 1995. Characteristics of the excitation and propagation of Lg from earthquakes in central Asia, in *Abstracts from the Seventh Annual IRIS Workshop*, 21-24 June 1995, Grand Teton National Park, WY.

Cong, L., Xie, J. and B.J. Mitchell, 1995. Excitation and propagation of Lg in central Eurasia, in *Proc. 17th Seismic Symposium on Monitoring a Comprehensive Test Ban Treaty*, 172-181, 12-15 Sep. 1995, Radison Resort, Scottsdale, AZ.

Xie, J., Cong, L. & B.J. Mitchell, 1995, Systematic difference between the excitation of Lg by earthquakes and underground nuclear explosions, *EOS, Trans. AGU, 1995 Fall Meeting*, **76**, F365.